

# Linearized Localized Orthogonal Decomposition for Quasilinear Nonmonotone Elliptic PDE

Maher Khrais\*      Barbara Verfürth\*

## Abstract

In this paper, we propose and analyze a multiscale method for a class of quasilinear elliptic problems of nonmonotone type with spatially multiscale coefficient. The numerical approach is inspired by the Localized Orthogonal Decomposition (LOD), so that we do not require structural assumptions such as periodicity or scale separation and only need minimal regularity assumptions on the coefficient. To construct the multiscale space, we solve linear fine-scale problems on small local subdomains, for which we consider two different linearization techniques. For both, we present a rigorous well-posedness analysis and convergence estimates in the  $H^1$ -semi norm. We compare and discuss theoretically and numerically the performance of our strategies for different linearization points. Numerical experiments underline the theoretical findings and illustrate the applicability of the method.

**Keywords**— nonmonotone quasilinear problem; multiscale method; a priori error estimate; LOD.

**AMS subject classifications**— 65N30, 65N15, 35J60, 65J15, 65N12

## 1 Introduction

Many applications lead to partial differential equations with *nonlinearities* and spatially *multiscale* coefficients. This includes stationary Richards equation in the context of groundwater flow [5]

or heat conductivity of modern composite materials [20]. Nonlinear models are considered to accurately model the physical responses of these materials, in particular at high temperatures, intensities or forces, where standard linear approximations are no longer valid. In addition, spatial multiscale coefficients model the heterogeneity of the media. This occurs in engineered composites as well as in nature. For instance, the conductivity in soil formations may change drastically over small distances.

In this work, we focus on a class of nonmonotone quasilinear elliptic PDEs of the form

$$-\nabla \cdot (\alpha(x, u)\nabla u) = f \quad \text{in } \Omega \tag{1}$$

in an open bounded domain  $\Omega \subset \mathbb{R}^d$ , where  $d \leq 3$ . Boundary conditions and detailed assumptions on  $\alpha$  will be made precise below. In general, the standard numerical approaches fail to describe in a satisfactory way the macro-scale behavior of the solution in the presence of high heterogeneity. In such approaches, the fine spatial features characterized by the parameter  $\varepsilon$  are difficult to resolve in the nonasymptotic regime, i.e., when the mesh size  $H$  satisfies  $H > \varepsilon$ .

To recover the optimal convergence rate w.r.t.  $H^1$ -norm,  $H$  must satisfy  $H \ll \varepsilon$ . However, such a numerical simulation would be prohibitively expensive.

The macroscopic behavior of the solution can be rigorously described by mathematical homogenization theory. In the limit  $\varepsilon \rightarrow 0$ , one may replace the original multiscale problem with the homogenized problem, whose coefficients are only slowly varying with respect to space. Mathematical homogenization of (1) has been studied in several papers, for example [16]. Generally

---

\*Institut für Numerische Simulation, Universität Bonn, Friedrich-Hirzebruch-Allee 7, D-53115 Bonn, Germany

speaking, numerical homogenization methods are mainly based on a macroscopic solver where missing macroscopic data (similar to the homogenized tensor) or suitable non-polynomial multiscale basis functions are obtained through microscopic solvers on local subdomains. Several numerical homogenization techniques have been proposed in the past few decades, especially for linear elliptic problems, see [9, 19, 25, 13], but the literature for nonlinear problems, in particular of nonmonotone type (1), is much more sparse.

The analysis and the applicability of the heterogeneous finite element method has been formulated and analyzed for the nonmonotone nonlinear elliptic problem (1) in [2, 10]. The numerical approach based on the multiscale finite element method MsFEM is studied for (1) with monotonicity assumption imposed on the coefficient in order to derive a convergence rate in [12]. The generalized multiscale FEM (GMsFEM) technique is implemented and analyzed to solve nonlinear elliptic problems in [14]. In the case of non-stationary Richard equations, the linearized system is tackled by utilizing constraint energy minimizing GMsFEM (CEM-GMsFEM) to obtain proper offline multiscale basis functions, see [22]. Relying on the partition of unity method to devise a global approximation spaces from local reduced space, a component-based parametric model order reduction (CB-pMOR) technique is proposed for the parametrized nonmonotone version of problem (1) in [26].

In this work, we consider a numerical homogenization approach inspired by the Localized Orthogonal Decomposition method (LOD), which has already successfully been applied to a range of (linear) problems, see [3, 25] for an overview. The goal of the LOD method is to incorporate the (spatial) fine-scale behavior of the coefficient  $\alpha$  into the basis of the coarse FE space resulting in a new modified low-dimensional function space with good approximation properties. The fine-scale incorporation into the coarse FE space is obtained by using correction operators. This operator is computed in a localized fashion on small patches of coarse mesh elements. However, these arguments cannot easily be transferred to the nonlinear case. For semilinear equations, the nonlinearity can be neglected in the construction of the correction operators because it is in a lower order term, see [17]. For quasilinear problems of monotone type, a multiscale method was proposed and analyzed in [27] which uses a linearization of the problem to compute the correction operators. The idea of linearization was later combined with an update strategy in [24] for nonlinear Helmholtz equations. Such an iterative numerical homogenization method, but based on generalized polyharmonic splines, is studied in [21] for a certain class of quasilinear monotone PDE.

In this work, we consider the original idea from [27] and once construct and compute a multiscale approximation space in a linearized fashion. This space is employed for the nonlinear multiscale problem with a Galerkin approach, which in practice of course uses an iterative method. We focus on the construction of the multiscale space and, in particular, on the linearization techniques involved for our nonmonotone PDE (1). This nonmonotone nature requires several changes in the design of the method and, in particular, its error analysis. Our main contribution is thus to extend the ideas from [27] to (1), which is a non-trivial task. Our a priori error estimate is of optimal order with respect to the mesh size without any dependence on the spatial variations of  $\alpha$  or (higher) regularity of the exact solution. Essentially, the error splits into a discretization error similar to the linear case and a linearization error, which we then further analyze. This gives guidance for the choice of the linearization point for the correction problems.

The paper is structured as follows. In the rest of Section 1, we introduce the model problem and summarize some essential findings on the existence and uniqueness of the solution and its finite element approximation. In Section 2, we introduce our multiscale approach and the linearization techniques that are needed for the correction computation. Section 3 is dedicated to the detailed and rigorous error analysis of our numerical method. We also discuss the linearization error and its impact on the error estimate. We finally present several numerical experiments in Section 4. These experiments underline the theoretical results and discuss the impact of the linearization points on the error.

**Notations:** Throughout the article, we use standard notation on Lebesgue and Sobolev spaces and their norms. For a given subdomain  $\Omega_1 \subseteq \Omega$ , let  $\|\cdot\|_{1,\Omega_1}$ ,  $\|\cdot\|_{1,\Omega_1}$ ,  $\|\cdot\|_\infty$ , and  $\|\cdot\|_{0,\Omega_1}$  denote the  $H^1(\Omega_1)$ -semi-norm, the standard  $H^1(\Omega_1)$ -norm, the  $L^\infty$ -norm, and the standard  $L^2(\Omega_1)$ -norm, respectively. The scalar product  $(\cdot, \cdot)_{\Omega_1}$  is the  $L^2$  inner product on the subdomain  $\Omega_1$ . We will omit the subscript  $\Omega_1$  if it is the full domain, i.e.,  $\Omega_1 = \Omega$ . We write  $a \lesssim b$  if there is a generic constant  $C$  (independent from the discretization and multiscale parameters) such that  $a \leq Cb$ . We also denote the derivative of the coefficient  $\alpha$  w.r.t. the second argument by  $\alpha_s$ .

## 1.1 Problem formulation

In this paper, we consider the following quasilinear nonmonotone elliptic problem

$$\begin{aligned} -\nabla \cdot (\alpha(x, u) \nabla u) &= f \text{ in } \Omega, \\ u &= 0 \text{ on } \partial\Omega. \end{aligned} \quad (2)$$

We assume homogeneous Dirichlet boundary conditions for simplicity. Other types of boundary conditions can be treated in a very similar manner. The matrix-valued coefficient  $\alpha(x, u) \in \mathbb{R}^{d \times d}$  encodes the properties of the material, in particular, we implicitly assume that it shows rapid oscillations on fine spatial scales. Therefore, we do not assume more than  $L^\infty$ -regularity of  $\alpha$  w.r.t.  $x$ , but some additional assumptions w.r.t. the nonlinearity are required to guarantee the well-posedness of problem (2).

**Assumption 1.** *Suppose that*

- $\alpha(x, s)$  is uniformly Lipschitz continuous w.r.t. the second argument, i.e., there exists  $\Lambda_0 > 0$  such that

$$|\alpha(x, s_1) - \alpha(x, s_2)| \leq \Lambda_0 |s_1 - s_2|, \quad \forall x \in \Omega, \quad s_1, s_2 \in \mathbb{R}. \quad (3)$$

- $\alpha(x, s)$  satisfies the uniform ellipticity and boundedness conditions, i.e., there exist  $\lambda > 0$ , and  $\Lambda_1 > 0$  such that

$$\alpha(x, s) \psi \cdot \psi \geq \lambda \|\psi\|^2, \quad \text{and} \quad \|\alpha(x, s) \psi\| \leq \Lambda_1 \|\psi\| \quad \forall x \in \Omega, \quad s \in \mathbb{R}, \quad \psi \in \mathbb{R}^d. \quad (4)$$

- for Fréchet linearization error analysis below, we impose the additional assumption that  $\alpha(x, s)$  is twice differentiable w.r.t. the second argument. Note that this assumption is not necessary to formulate our method.

In addition, we assume that  $f \in L^2(\Omega)$ . Now, consider the weak formulation of finding  $u \in H_0^1(\Omega)$  that solves

$$\mathcal{A}(u; u, v) := (\alpha(x, u) \nabla u, \nabla v) = (f, v) = F(v), \quad \forall v \in H_0^1(\Omega). \quad (5)$$

Given Assumption 1, for any  $q \in H_0^1(\Omega)$ , the bilinear form  $\mathcal{A}(q; \cdot, \cdot)$  inherits the ellipticity and boundedness conditions in  $H_0^1(\Omega)$ , i.e., there exists  $\lambda > 0$  and  $\Lambda_1 > 0$  such that

$$\begin{aligned} \lambda |w|_1^2 &\leq \mathcal{A}(q; w, w), \quad \forall q, w \in H_0^1(\Omega), \\ \mathcal{A}(q; v, w) &\leq \Lambda_1 |v|_1 |w|_1, \quad \forall q, v, w \in H_0^1(\Omega). \end{aligned}$$

Hence, one can ensure the existence and the uniqueness of the solution  $u \in H_0^1(\Omega)$  of the weak problem (5) such that

$$\mathcal{A}(u; u, v) = F(v), \quad \forall v \in H_0^1(\Omega). \quad (6)$$

The weak solution  $u$  satisfies

$$|u|_1 \leq C \|f\|_0, \quad (7)$$

where  $C$  depends on the constants of (4) in Assumption 1, but is independent of the spatial variation of  $\alpha$  [6]. We refer to [6, 8, 18] for the proof of existence and uniqueness of the weak solution of problem (5).

## 1.2 Finite element method

Consider a decomposition of the domain of interest  $\Omega$  into a partition  $\mathcal{T}_H$  of simplices or quadrilaterals. Let  $K$  denote the elements of  $\mathcal{T}_H$  and the corresponding diameter  $H_K$ , assume

$$H := \max_{K \in \mathcal{T}_H} H_K.$$

We assume that  $\mathcal{T}_H$  is shape-regular and quasi-uniform.

We emphasize that  $\mathcal{T}_H$  is coarse in the sense that it does not recover the spatial variation of  $\alpha$ . Let  $V_H$  be the standard lowest-order conforming finite element subspace of  $H_0^1(\Omega)$ . It consists of piecewise polynomials of total degree at most 1, if  $K$  is a simplex, or of partial degree at most

1 in each variable, if  $K$  is quadrilateral. The finite element method seeks to find the solution  $u_H \in V_H$  that satisfies

$$\mathcal{A}(u_H; u_H, v_H) = (f, v_H) \quad \forall v_H \in V_H.$$

In practice, the arising nonlinear system is solved using an appropriate iterative method, e.g. the Newton method. The heterogeneity of  $\alpha(x, u) \in \mathbb{R}^{d \times d}$  w.r.t.  $x$  needs to be considered when solving (5) numerically. In order to have an accurate approximation solution that recovers the main properties of the solution  $u$ , the triangulation  $\mathcal{T}_H$  should capture all the features of the medium. In practice the mesh size  $H$  needs to be small enough. This assumption is crucial to guarantee the desired convergence order. However, that would lead to a computationally expensive method. In addition, the uniqueness of the approximation solution is not trivial, even though the weak problem itself admits a unique solution in  $H_0^1(\Omega)$  [4]. Given the regularity assumption of the weak solution, the uniqueness of the approximation solution is addressed in [1] for general order of the finite-dimensional function space  $l \geq 1$ . It is proved that the error in the  $H^1$  semi-norm fulfills

$$|u - u_H|_1 \leq CH^l,$$

given that  $u \in H^{l+1}(\Omega)$ . With some extra assumptions on the regularity of the given data, the convergence w.r.t.  $L^2$  is shown to be

$$\|u - u_H\|_0 \leq C_2 H^{l+1},$$

where the constant  $C_2$  is independent of the mesh size  $H$ . For our case  $l = 1$ , we need at least  $u \in H^2(\Omega)$  for the above estimate. However, this is not always guaranteed as the coefficient  $\alpha$  may be discontinuous w.r.t.  $x$ . Moreover, even if  $u \in H^2(\Omega)$ , the constants  $C$  and  $C_2$  depend on the spatial variations of  $\alpha$ , which is not desirable for multiscale coefficient. Here, we will employ the LOD method to achieve optimal convergence rate without dependency on the mesh size and without requiring more than  $u \in H_0^1(\Omega)$ .

## 2 Multiscale method

In this section, we introduce our multiscale method using basis functions which are computed from localized and linearized versions of problem (5). This is largely inspired by the multiscale method for quasilinear monotone problem in [27], which in turn is inspired by the Localized Orthogonal Decomposition (LOD) [25]. The key aim is to identify a low-dimensional subspace of  $H_0^1(\Omega)$  with good approximation properties for the multiscale problem. This is done by a decomposition of  $H_0^1(\Omega)$  into coarse and fine orthogonal subspaces. In the nonlinear case, we still have to identify the appropriate form of orthogonality, see below. Next, we discuss the key aspect of the LOD approach. We describe the orthogonal decomposition of the space  $H_0^1(\Omega)$  and the steps involved. In addition, we outline the linearization procedures used to address the nonlinearity when solving the correction problems. That is required to construct the orthogonal multiscale space linearly. Finally, we explain the localization strategies employed to construct the space of interest locally.

### 2.1 (Orthogonal) Decompositions

The first attempt to decompose  $H_0^1(\Omega)$  into orthogonal subspaces depends mainly on using a suitable interpolation operator that satisfies certain properties. More precisely, let  $I_H : H_0^1(\Omega) \rightarrow V_H$  be a bounded local linear projective operator, i.e.,  $I_H(v_H) = v_H \quad \forall v_H \in V_H$  that additionally satisfies the following stability and the approximation properties

$$|I_H v|_{1,K} \lesssim |v|_{1,N(K)}, \quad \|v - I_H v\|_{0,K} \lesssim H |v|_{1,N(K)}, \quad (8)$$

for all  $v \in H_0^1(\Omega)$ , where  $N(K)$  is the union of elements that have nonempty intersection with the element  $K$ . An example of projective interpolation that is commonly used in the LOD literature is defined as follows

$$I_H : H_0^1(\Omega) \xrightarrow{\Pi_H} S^1(\mathcal{T}_H) \xrightarrow{E_H} V_H,$$

where  $\Pi_H$  is the  $L^2$  projection onto the elementwise affine functions  $S^1(\mathcal{T}_H)$ , and  $E_H$  is an averaging operator. This choice is not restrictive, one can use any projective interpolation that satisfies the stability and approximation properties in (8). Practically, we only require the kernel of the projection for the implementation of LOD. Given  $I_H$  that satisfies the properties

mentioned above in (8), the space  $W = \ker I_H$  contains all so-called fine-scale functions that cannot be captured in the finite element functions space  $V_H$ . Due to the projection property of the interpolation  $I_H$ , the space  $H_0^1$  can be uniquely decomposed as follows

$$H_0^1 = V_H \oplus W.$$

This decomposition does not depend on the problem formulation. For the linear case, the idea of the LOD is to consider another decomposition  $H_0^1 = V_H^{\text{ms}} \oplus W$  that is orthogonal w.r.t. the energy scalar product of the problem. If one tries to transfer the idea to the present nonlinear case, one might try to define the space  $V_H^{\text{nl,ms}}$  via

$$\mathcal{A}(v_H^{\text{nl,ms}}; v_H^{\text{nl,ms}}, w) = 0, \quad \forall v_H^{\text{nl,ms}} \in V_H^{\text{nl,ms}}, \quad \forall w \in W. \quad (9)$$

However, this is a nonlinear “space” because of the nonlinearity of  $\mathcal{A}$ . This can, in particular, be seen when one tries to write it in the usual form  $V_H^{\text{nl,ms}} = (\text{id} - Q^{\text{nl}})V_H$ , where  $Q^{\text{nl}} : V_H \rightarrow W$  is a nonlinear so-called correction operator. The nonlinearity of  $Q^{\text{nl}}$  as well as  $V_H^{\text{nl,ms}}$  complicates the multiscale method due to the coupling of the nonlinear problem (9) to construct the space and the resulting nonlinear problem from the Galerkin approach. In particular, it is not straightforwardly clear that such a multiscale method is well-defined. Instead, we will discuss a linearized construction of multiscale basis functions in the following.

## 2.2 Linearizations

Here, we introduce two possible linearization methods for  $\mathcal{A}$  that we will use to formulate linearized corrector problems in the next subsection. The linearization approximation of the nonlinearity of  $\alpha(x, u)\nabla u$  is of the following abstract form

$$\mathbf{A}_L(x, p^*, \nabla v) = \alpha_L(x, p^*)\nabla v + C_L(x, p^*),$$

where  $p^*$  is an a priori chosen, fixed function that we call the linearization point. Two possible techniques that we consider in this article are

- **Kačanov-type** linearization, which “freezes” the nonlinearity in  $\alpha$  at the linearization point  $p^*$ , i.e.,

$$\mathbf{A}_L(x, p^*, \nabla v) = \alpha(x, p^*)\nabla v.$$

Note that this means that  $\alpha_L(x, p^*) = \alpha(x, p^*)$  and  $C_L(x, p^*) = 0$  in the abstract form.

- **Fréchet derivative** linearization, which is inspired by the Newton method. The Fréchet derivative at the linearization point  $p^*$  in the direction of  $u - p^*$  reads

$$\mathcal{F}(p^*)(u - p^*) = \alpha(x, p^*)\nabla(u - p^*) + (u - p^*)\alpha_s(x, p^*)\nabla p^*.$$

To simplify the presentation and the computation of the corrector, we may remove the constant  $\alpha(x, p^*)\nabla p^*$  that does not affect the correction computation, so we have the following linearization formula

$$\mathbf{A}_L(x, p^*, \nabla v) = \alpha(x, p^*)\nabla v + (v - p^*)\alpha_s(x, p^*)\nabla p^*,$$

where we replaced  $u$  by (general)  $v$ . Note that  $\mathbf{A}_L$  is affine in  $\nabla v$  with a non-zero constant term. In the abstract form, it corresponds to  $\alpha_L(x, p^*) = \alpha(x, p^*)$  and  $C_L(x, p^*) = \alpha_s(x, p^*)\nabla p^*$ .

## 2.3 Localized correction operators

We now want to apply our linearization strategies from above to formulate the localized correctors  $Q : V_H \rightarrow W$ . In order to guarantee the well-posedness of the corrector problems, we require the following assumption on  $\mathbf{A}_L(x, p^*, \nabla v)$ . Note that for the above presented linearization strategies, these assumptions are inherited from Assumption 1 for the original problem.

**Assumption 2.** *Suppose that*

- $\alpha_L(x, p^*) \in L^\infty(\Omega, \mathbb{R}^{d \times d})$  and  $C_L(x, p^*) \in L^2(\Omega, \mathbb{R})$ ,  $\forall p^* \in H_0^1(\Omega)$ .

- there exists  $0 < \lambda_L < \Lambda_L$  such that

$$\lambda_L |\psi|^2 \leq \alpha_L(x, p^*) \psi \cdot \psi \leq \Lambda_L |\psi|^2, \quad \forall x \in \Omega, p^* \in H_0^1(\Omega), \psi \in \mathbb{R}^d.$$

We define the corrector operator  $Q : V_H \rightarrow W$  via

$$\mathcal{A}_L(p^*, v_H - Qv_H, w) = 0, \quad \forall v_H \in V_H \text{ and } \forall w \in W, \quad (10)$$

where the bilinear form  $\mathcal{A}_L$  is defined as

$$\mathcal{A}_L(p^*, v_1, v_2) = (\mathbf{A}_L(x, p^*, \nabla v_1), \nabla v_2)_\Omega.$$

The linearization  $\mathbf{A}_L(x, p^*, \nabla v_1)$  was introduced above and incorporates our two models, the Kačanov-type and Fréchet derivative linearization. Due to  $C_L = 0$ , Assumption 2 directly yields the well-posedness of the corrector problem for the Kačanov-type linearization. The well-posedness in the case of Fréchet derivative will be addressed and analyzed in Subsection 3.2. The ideal multiscale method is now a Galerkin method based on  $V_H^{\text{ms}} = (\text{id} - Q)V_H$ , which is now a linear space, such that the method is indeed well-defined. We still call this method ideal because the correction operator  $Q$  has global support for  $d > 1$ . In the linear case, [25] shows that the correction  $Q$  decays exponentially away from the element of interest, we refer to proposition 2. Note that these results can also be applied to our *linearized* corrector problems. Hence, we localize the corrector  $Q$  by truncating the domain of computation as detailed in the next subsection.

## 2.4 Localization and practical method

In this subsection we introduce the localization of the global correction problem (10). We first need some additional notation. Let  $N^k(T)$  denote the  $k$ -layer patch of neighboring elements of the element  $T$  which is defined in an inductive manner as follows

$$N^0(T) = T, \quad N^k(T) = \bigcup_{\substack{K \in \mathcal{T}_H \\ \overline{K} \cap N^{k-1}(T) \neq \emptyset}} K.$$

The parameter  $k$  represents the degree of localization of the corrector because it determines the size of the patch. The quasi-uniformity assumption of  $\mathcal{T}_H$  ensures that size of elements that belong to  $k$ -layer patches is bounded by a constant  $C_{\text{ol}}$  that only depends on  $k$  in a polynomial manner, i.e.,

$$\max_{T \in \mathcal{T}_H} |\{K \in \mathcal{T}_H : K \in N^k(T)\}| \leq C_{\text{ol}}. \quad (11)$$

Now, we define the localized correction operator as

$$Q^k : V_H \rightarrow W, \quad Q^k = \sum_{T \in \mathcal{T}_H} Q_{T,k},$$

where

$$Q_{T,k} : V_H \rightarrow W(N^k(T)) := \{w \in W : \text{supp}(w) \subseteq \overline{N^k(T)}\}.$$

The local correction problem reads as follows: Find the correction  $Q_{T,k}v_H \in W(N^k(T))$  of  $v_H \in V_H$  that satisfies

$$(\mathcal{A}_L)_{N^k(T)}(p^*, Q_{T,k}v_H, w) = (\mathcal{A}_L)_T(p^*, v_H, w), \quad \forall w \in W(N^k(T)). \quad (12)$$

Here, the bilinear forms on the left-hand side and right-hand side are restricted to the subdomains  $N^k(T)$  and  $T$ , respectively.

To construct our multiscale space, we replace  $Q$  by  $Q_k$  and define

$$V_{H,k} = (\text{id} - Q^k)V_H = \{v_H - Q^k v_H : v_H \in V_H\}.$$

Note that  $V_{H,k}$  is constructed by correcting the basis of the space  $V_H$ . Finally, we formulate our Galerkin method on  $V_{H,k}$  as follows: Find  $u_{H,k} \in V_{H,k}$  that satisfies

$$\mathcal{A}(u_{H,k}; u_{H,k}, v_{H,k}) = (f, v_{H,k}), \quad \forall v_{H,k} \in V_{H,k}. \quad (13)$$

Observe that we solve the nonlinear problem on the low-dimensional space  $V_{H,k}$ . The localization procedure above affects only the space construction, but not the final problem. In practice, then again one uses an iterative method to solve the associated nonlinear system.

**Remark 1.**

- As we discussed before for the finite element method, uniqueness of the approximate solution  $u_{H,k} \in V_{H,k}$  for problem (2) is only guaranteed for sufficiently fine meshes, i.e., there is  $H_0$  such that for any  $H \leq H_0$ , we have a unique solution  $u_{H,k} \in V_{H,k}$ . We refer to [4, 7, 1] and the reference therein for further arguments and details. The error analysis below, however, does not require uniqueness of  $u_{H,k}$ , but holds for any discrete solution. In practice, we did not experience any issues with non-uniqueness.
- One can also consider a Petrov-Galerkin formulation of the LOD to reduce the communication between the correctors. This means to find  $u_{H,k}^{PG} \in V_{H,k}$  such that

$$\mathcal{A}(u_{H,k}^{PG}; u_{H,k}^{PG}, v_H) = (f, v_H), \quad \forall v_H \in V_H.$$

- The corrector problems (12) are still posed on infinite dimensional subspaces  $W(N^k(T))$ , which need to be discretized. This is accomplished as usual by introducing a fine-scale mesh  $\mathcal{T}_h$  of  $\Omega$  with elements  $K$  of diameter  $h_K$ . Let  $h := \max_{K \in \mathcal{T}_h} h_K$  such that  $h \ll H$  resolves all features of  $\alpha$ . Let  $V_h$  be the lowest order Lagrange finite element space associated with  $\mathcal{T}_h$ . Consider the following fine-scale space

$$W_h(N^k(T)) := \{w_h \in V_h \cap W : \text{supp}(w_h) \subseteq \overline{N^k(T)}\}.$$

In practice, the corrector problem (12) is solved with the new fine-scale space  $W_h(N^k(T))$ .

### 3 Error Analysis

In this section, we present the error analysis of the multiscale approach introduced in Section 2. Specifically, we outline the analysis for the two linearization strategies used in the correction computations, demonstrate the behavior of the linearization method, and examine the impact of the linearization points on the convergence rate. Assume that we have a fixed linearization point  $p^* \in H_0^1(\Omega)$  and fixed tensor  $\alpha(x, p^*)$  w.r.t. the second argument. The effect of localizing the correction problems is quantified as follows.

**Proposition 2.** *Let Assumptions 1 and 2 be satisfied. Let  $Q$  be the linear corrector defined in (10) and its localized version  $Q^k$  defined in (12). There exists constant  $0 < \nu < 1$  such that for any  $v_H \in V_H$ , the following inequality is satisfied*

$$|(Q - Q^k)v_H|_1 \lesssim C_{\text{ol}}^{\frac{1}{2}} \nu^k |v_H|_1,$$

where  $C_{\text{ol}}$  is the constant in (11).

The proposition above is proved in [25] for the case of linear elliptic problem, where the correction problems are also linear elliptic. We will discuss its validity for the linear corrector problems (12) in the proofs below. The proposition shows that the error between the corrector operator and its local version decays exponentially in the number of layers. We essentially split the error of the multiscale method into a localization contribution and the error of the ‘‘ideal’’ method with  $Q$ . To estimate the latter, we need to additionally quantify the error from the linearization of the correction problems. Given  $v \in H_0^1(\Omega)$  and for a fixed linearization point  $p^* \in H_0^1(\Omega)$ , we define the linearization error corresponding to the nonlinear form  $\alpha(x, v)\nabla v$  as

$$\eta(v) = \sup_{w \in H_0^1(\Omega), |w|_1=1} \left| \int_{\Omega} [\alpha(x, v)\nabla v - \mathbf{A}_L(x, p^*, \nabla v)] \cdot \nabla w dx \right|.$$

We can now formulate our main result.

**Theorem 3.** *Let Assumptions 1 and 2 be satisfied. Let  $u$  be the solution to (5), and let  $u_{H,k}$  be the multiscale solution to (13). Then it holds that*

$$|u - u_{H,k}|_1 \lesssim (H + C_{\text{ol}}^{\frac{1}{2}} \nu^k) \|f\|_0 + G(u - p^*, u_{H,k} - p^*),$$

where  $G(u - p^*, u_{H,k} - p^*)$  satisfies the following inequalities:

(a) *Kačanov-type linearization*

$$G(u - p^*, u_{H,k} - p^*) \lesssim \|u - p^*\|_\infty \|\nabla u\|_0 + \|\nabla u_{H,k}\|_0 \|u_{H,k} - p^*\|_\infty.$$

(b) *Fréchet derivative linearization*

$$\begin{aligned} G(u - p^*, u_{H,k} - p^*) &\lesssim \|u - p^*\|_\infty \|\nabla u\|_0 + \|\nabla u_{H,k}\|_0 \|u_{H,k} - p^*\|_\infty \\ &\quad + \|(\alpha_{ss}(x, q^*) \nabla q^*)\|_\infty \|u - p^*\|_0^2, \end{aligned}$$

where  $q^* \in H_0^1(\Omega)$  is an intermediate function, i.e.,  $q^* = p^* + t(u - p^*)$ , for some  $t \in [0, 1]$ .

The above theorem shows that we achieve a convergence of first order up to the linearization error. For both strategies, the errors are identical with an extra term in the case of Fréchet linearization, that is due to the additional convection term in the Fréchet derivative. The order of convergence above is also compatible with the results obtained in [27] for the monotone nonlinear problem up to the linearization error. In the corollary below, we estimate the error for the finite element part of the LOD solution, namely,  $I_H u_{H,k}$ .

**Corollary 4.** *Let Assumptions 1 and 2 be satisfied. Let  $u$  be the solution of (5) and let  $u_{H,k}$  be the LOD solution of (13). Then we have*

$$\|u - I_H u_{H,k}\|_0 \lesssim \|u - I_H u\|_0 + \|u - u_{H,k}\|_0 + H|u - u_{H,k}|_1. \quad (14)$$

*Proof of Corollary 4.* By triangle inequality and the approximation property of  $I_H$  we have that

$$\|u - I_H u_{H,k}\|_0 \leq \|u - I_H u\|_0 + \|I_H u - I_H u_{H,k}\|_0.$$

Using the stability and approximation of the interpolation  $I_H$ , and Poincaré inequality, we obtain for the second term that

$$\begin{aligned} \|I_H u - I_H u_{H,k}\|_0 &\lesssim \|u - u_{H,k} - (u - u_{H,k}) + I_H u - I_H u_{H,k}\|_0, \\ &\lesssim \|u - u_{H,k}\|_0 + H|u - u_{H,k}|_1. \end{aligned} \quad \square$$

The error estimate of Corollary 4 can be further refined if the  $L^2$  estimate  $\|u - u_{H,k}\|_0$  is available (it should be  $O(H^2)$  by Aubin-Nitsche trick). Hence, with the estimate of the first and last term in (14) and if  $k \approx |\log(H)|$ , it yields an estimate that is at least of the first order up to the linearization error and even of order  $H^2$  if  $u$  is sufficiently regular. Furthermore, the term  $\|u - I_H u\|_0$  can be estimated against the  $L^2$ -best-approximation error of  $V_H$  if we assume  $L^2$  stability of  $I_H$ , i.e.,  $\|I_H v\|_0 \lesssim \|v\|_0 \forall v_H \in V_H$ , the estimate (14) can be rewritten as

$$\|u - I_H u_{H,k}\|_0 \lesssim \inf_{v_H \in V_H} \|u - v_H\|_0 + \|u - u_{H,k}\|_0.$$

The  $L^2$ -best-approximation error converges at least  $O(H)$  for  $u \in H_0^1(\Omega)$ , and even better rates are possible if we assume more regularity of  $u$ .

**Remark 5.** *We discuss some implications of the above error estimates.*

- *Note that the upper bound in the error analysis depends on the infinity norm of both errors, namely  $\|u - p^*\|_\infty$  and  $\|u_{H,k} - p^*\|_\infty$ . This suggests that the linearization point  $p^*$  should be carefully selected close to  $u$  and  $u_{H,k}$  at the same time to ensure that  $G(u - p^*, u_{H,k} - p^*)$  is sufficiently small. Then, we obtain the first order of convergence w.r.t.  $H$ , if the size of the patch satisfies  $k \approx \log(H)$ .*
- *To specify a good selection for the linearization points, observe the term  $\|\nabla u_{H,k}\|_0 \|u_{H,k} - p^*\|_\infty$  can be evaluated a posteriori. We therefore mainly focus on suitable choice of  $p^*$  that can make the value of  $\|u - p^*\|_\infty$  very small. We will further discuss the choice of the linearization in Section 4.*
- *We point out that the generic constants in the analysis above are independent of the mesh size and the spatial variations of  $\alpha$  and mainly depend on the constants in the Assumptions 1 and 2 and also on the constant  $C_{01}$ .*



- From a theoretical point of view, no significant difference is expected between both linearization approaches, provided that the linearization point is chosen carefully to be close to both solutions. However, we observe a slight yet important difference between the two methods. In the case of Fréchet derivative linearization, it is crucial to choose the linearization point carefully in such a way the conditions  $\|\alpha_s(x, p^*)\nabla p^*\|_\infty \leq C_{p^*}$  and  $C_I C_{p^*} H < 1$  are satisfied to ensure the convergence and ellipticity and consequently the well-posedness as we will discuss below. In contrast, there is no such condition for the case of Kačanov linearization.

In the following analysis, we split our explanations into two subsections based on the linearization technique. We first present the analysis for the case of using Kačanov technique and then proceed with the analysis for the case of Fréchet derivative.

### 3.1 Error analysis for Kačanov-type linearization

Kačanov linearization model ends up with a linear elliptic problem that inherits the assumptions of coercivity and boundedness. As a result, the correction problem (12) is well-posed. Moreover, the inherited ellipticity assumption ensures the validity of the exponential decaying error in Proposition 2 for the correctors that are computed using the bilinear form defined by the Kačanov technique.

*Proof of Theorem 3(a).* By triangle inequality, we have for any  $v_{H,k} \in V_{H,k}$

$$|u - u_{H,k}|_1 \leq |u - v_{H,k}|_1 + |v_{H,k} - u_{H,k}|_1. \quad (15)$$

We now specifically choose  $v_{H,k} = (\text{id} - Q^k)I_H u = (\text{id} - Q)I_H u + (Q - Q^k)I_H u$ . First, we bound the first term on the right-hand side of (15) as follows

$$|u - v_{H,k}|_1 \leq |u - (\text{id} - Q)I_H u|_1 + |(Q - Q^k)I_H u|_1. \quad (16)$$

The second term is bounded using Proposition 2, the stability assumptions of the interpolation, and (7) to yield

$$|(Q - Q^k)I_H u|_1 \lesssim C_{01}^{\frac{1}{2}} \nu^k \|f\|_0.$$

To bound the first term of (16), let  $\xi = (\text{id} - Q)I_H u$ . Using (5) for the solution  $u$ , the uniform ellipticity of  $\alpha(x, v)$  for all  $v \in H_0^1(\Omega)$ , the stability of the interpolation, and the orthogonality from (10), we obtain

$$\begin{aligned} |u - \xi|_1^2 &\lesssim \int_{\Omega} \alpha(x, p^*) \nabla(u - \xi) \cdot \nabla(u - \xi) dx = \int_{\Omega} (\alpha(x, p^*) \nabla u - \alpha(x, p^*) \nabla \xi) \cdot \nabla(u - \xi) dx \\ &= \int_{\Omega} (\mathbf{A}_L(x, p^*, u) - \mathbf{A}_L(x, p^*, \xi)) \cdot \nabla(u - \xi) dx \\ &= \int_{\Omega} [\mathbf{A}_L(x, p^*, u) - \alpha(x, u) \nabla u + \alpha(x, u) \nabla u] \cdot \nabla(u - \xi) dx \\ &\lesssim (H \|f\|_0 + \eta(u)) |u - \xi|_1. \end{aligned}$$

In the last inequality, we have used that  $u - \xi \in W$ . Together with the approximation property of  $I_H$ , we obtain the following first order of convergence

$$\begin{aligned} |(f, u - \xi)_0| &\leq \|f\|_0 \|u - \xi\|_0 = \|f\|_0 \|u - \xi - I_H(u - \xi)\|_0 \\ &\leq H \|f\|_0 |u - \xi|_1. \end{aligned}$$

Second, to estimate the second term of (15), Observe that since both  $u$  and  $u_{H,k}$  are solutions to (5) and (13) respectively, we have that

$$\int (\alpha(x, u) \nabla u - \alpha(x, u_{H,k}) \nabla u_{H,k}) \nabla \psi_{H,k} = 0$$

for any test function  $\psi_{H,k} \in V_{H,k}$ . This identity with the ellipticity and boundedness as well as the Lipschitz continuity of  $\alpha(x, v)$  for all  $v \in H_0^1(\Omega)$  yields

$$\begin{aligned}
|v_{H,k} - u_{H,k}|_1^2 &\lesssim \int_{\Omega} \alpha(x, p^*) \nabla(v_{H,k} - u_{H,k}) \cdot \nabla(v_{H,k} - u_{H,k}) dx \\
&\leq \int_{\Omega} (\alpha(x, p^*) \nabla v_{H,k} - \alpha(x, u) \nabla v_{H,k} + \alpha(x, u) \nabla v_{H,k} - \alpha(x, u) \nabla u \\
&\quad + \alpha(x, u_{H,k}) \nabla u_{H,k} - \alpha(x, p^*) \nabla u_{H,k}) \cdot \nabla(v_{H,k} - u_{H,k}) dx \\
&\leq \|\alpha(x, p^*) \nabla v_{H,k} - \alpha(x, u) \nabla v_{H,k} + \alpha(x, u) \nabla v_{H,k} - \alpha(x, u) \nabla u \\
&\quad + \alpha(x, u_{H,k}) \nabla u_{H,k} - \alpha(x, p^*) \nabla u_{H,k}\|_0 |v_{H,k} - u_{H,k}|_1 \\
&\leq (\Lambda_0 \|\nabla v_{H,k}\|_0 \|u - p^*\|_{\infty} + \Lambda_1 |u - v_{H,k}|_1 + \Lambda_0 \|\nabla u_{H,k}\|_0 \|u_{H,k} - p^*\|_{\infty}) \\
&\quad \cdot |v_{H,k} - u_{H,k}|_1 \\
&\lesssim (\|\nabla v_{H,k}\|_0 \|u - p^*\|_{\infty} + |u - v_{H,k}|_1 + \|\nabla u_{H,k}\|_0 \|u_{H,k} - p^*\|_{\infty}) |v_{H,k} - u_{H,k}|_1.
\end{aligned}$$

Inserting the previously obtained estimate for  $|u - v_{H,k}|_1$ , we have

$$|v_{H,k} - u_{H,k}|_1 \lesssim \|\nabla v_{H,k}\|_0 \|u - p^*\|_{\infty} + H \|f\|_0 + \eta(u) + C_{\text{ol}}^{\frac{1}{2}} \nu^k \|f\|_0 + \|\nabla u_{H,k}\|_0 \|u_{H,k} - p^*\|_{\infty}.$$

Finally, combining both estimates for  $|v_{H,k} - u_{H,k}|_1$  and  $|u - v_{H,k}|_1$  yields

$$|u - u_{H,k}|_1 \lesssim (H + C_{\text{ol}}^{\frac{1}{2}} \nu^k) \|f\|_0 + \eta(u) + \|\nabla v_{H,k}\|_0 \|u - p^*\|_{\infty} + \|\nabla u_{H,k}\|_0 \|u_{H,k} - p^*\|_{\infty}.$$

To further examine the linearization error  $\eta(u)$ , we utilize the Lipschitz continuity of the coefficient  $\alpha$ , which gives

$$\begin{aligned}
\eta(u) &\leq \|\alpha(x, p^*) \nabla u - \alpha(x, u) \nabla u\|_0 \\
&\leq \|\alpha(x, p^*) - \alpha(x, u)\|_{\infty} \|\nabla u\|_0 \\
&\lesssim \|p^* - u\|_{\infty} \|\nabla u\|_0.
\end{aligned}$$

Collecting all estimates, we see that it only remains to bound  $\|\nabla v_{H,k}\|_0$ . We use its definition and the stability of  $Q^k$  and  $I_H$  to obtain

$$\|\nabla v_{H,k}\|_0 = \|\nabla(\text{id} - Q^k)I_H u\|_0 \lesssim \|\nabla u\|_0. \quad \square$$

## 3.2 Error analysis for Fréchet derivative linearization

We now estimate the error in (15) in the case of linearizing the correction computations with the Fréchet derivative. First, we discuss the well-posedness of the correction problem and its exponential decay. In [23], the exponential decay of the correction operator is proved for general bilinear forms that satisfy an inf-sup condition satisfied on the fine-scale space  $W$  and its subspace  $W_{k,K}^c := \{w \in W : \text{supp}(w) \subseteq \Omega \setminus N^k(K)\}$ . Therefore, this ensures the uniqueness of the solution for the correction problem. For our case when using the Fréchet-type linearization, we show below the coercivity of  $\mathcal{A}_L$  on the space  $W$  for sufficiently small  $H$ . The same proof can also be applied for  $W_{k,K}^c$ .

Specifically, we need to assume that  $C_I C_{p^*} H < 1$ , where  $C_{p^*}$  is an upper bound such that  $\|\alpha_s(x, p^*) \nabla p^*\|_{\infty} \leq C_{p^*}$  and  $C_I$  is the constant of the interpolation estimate in (8). If  $\alpha$  is not only Lipschitz continuous, but even  $C^1$ -regular w.r.t. the second argument, such a constant  $C_{p^*}$  can always be found and depends on the choice of the (fixed) linearization point  $p^*$ . By the ellipticity of  $\alpha$ , we obtain for any  $w \in W$  that

$$\begin{aligned}
|w|_1^2 &\lesssim \int_{\Omega} (\alpha(x, p^*) \nabla w + w \alpha_s(x, p^*) \nabla p^*) \cdot \nabla w dx - \int_{\Omega} w \alpha_s(x, p^*) \nabla p^* \cdot \nabla w dx \\
&\lesssim (\mathcal{A}_L(p^*, w, w) + \|\alpha_s(x, p^*) \nabla p^*\|_{\infty} \|w\|_0) |w|_1 \\
&\lesssim (\mathcal{A}_L(p^*, w, w) + \|\alpha_s(x, p^*) \nabla p^*\|_{\infty} \|w - I_H w\|_0) |w|_1 \\
&\lesssim \mathcal{A}_L(p^*, w, w) + C_I C_{p^*} H |w|_1^2.
\end{aligned}$$

Hence, the bilinear form  $\mathcal{A}_L(p^*, w, w)$  is coercive under the assumption  $C_I C_{p^*} H < 1$ . This implies the well-posedness of the correction problem that is solved using Fréchet derivative as a linearization formula. Moreover, the exponential decay of  $Q$  as in Proposition 2 holds.

*Proof of Proposition 3(b).* Similar to the proof for part (a), we have (15) and choose

$$v_{H,k} = (\text{id} - Q^k)I_H u = (\text{id} - Q)I_H u + (Q - Q^k)I_H u.$$

First, we bound the first term on the right hand side of the inequality (15) as

$$|u - v_{H,k}|_1 \leq |u - (\text{id} - Q)I_H u|_1 + |(Q - Q^k)I_H u|_1. \quad (17)$$

As discussed above, Proposition 2 holds for sufficiently fine  $H$  so that we bound the second term similar to the Kačanov case.

Recall  $\xi = (\text{id} - Q)I_H u$ . To bound the first term of (17), we use the uniform ellipticity of the linearized tensor  $\alpha$ , the stability of the interpolation, and the orthogonality from (10) and obtain

$$\begin{aligned} |u - \xi|_1^2 &\lesssim \int_{\Omega} (\alpha(x, p^*) \nabla(u - \xi) + \alpha_s(x, p^*) \nabla p^*(u - \xi)) \cdot \nabla(u - \xi) dx \\ &\quad - \int_{\Omega} \alpha_s(x, p^*) \nabla p^*(u - \xi) \cdot \nabla(u - \xi) dx, \\ &= \int_{\Omega} (A_L(x, p^*, u) - \alpha(x, u) \nabla u + \alpha(x, u) \nabla u) \cdot \nabla(u - \xi) dx \\ &\quad - \int_{\Omega} \alpha_s(x, p^*) \nabla p^*(u - \xi) \cdot \nabla(u - \xi) dx \\ &\lesssim H \|f\|_0 |u - \xi|_1 + \eta(u) |u - \xi|_1 + \|\alpha_s(x, p^*) \nabla p^*\|_{\infty} \|u - \xi\|_0 |u - \xi|_1, \\ &\lesssim (H \|f\| + \eta(u) + \|\alpha_s(x, p^*) \nabla p^*\|_{\infty} \|u - \xi - I_H(u - \xi)\|_0) |u - \xi|_1, \\ &\lesssim (H \|f\|_0 + \eta(u) + C_I C_{p^*} H |u - \xi|_1) |u - \xi|_1. \end{aligned}$$

As mentioned before, we assume  $H$  to be sufficiently fine in the sense of  $C_I C_{p^*} H < 1$ , so we obtain

$$|u - \xi| \lesssim H \|f\|_0 + \eta(u).$$

Second, to prove the second term in (15), we follow the same steps of the proof of the Kačanov case and get

$$|v_{H,k} - u_{H,k}| \lesssim (\|\nabla v_{H,k}\|_0 \|u - p^*\|_{\infty} + H \|f\|_0 + \eta(u) + \|\nabla u_{H,k}\|_0 \|u_{H,k} - p^*\|_{\infty}) + C_{\Omega}^{\frac{1}{2}} \nu^k \|f\|_0.$$

Combining the two estimates yields

$$|u - u_{H,k}| \lesssim (H + C_{\Omega}^{\frac{1}{2}} \nu^k) \|f\|_0 + \|\nabla v_{H,k}\|_0 \|u - p^*\|_{\infty} + \eta(u) + \|\nabla u_{H,k}\|_0 \|u_{H,k} - p^*\|_{\infty}.$$

It remains to estimate the linearization error. Using the Taylor series expansion on  $\alpha(x, u) \nabla u$ , we obtain

$$\begin{aligned} \eta(u) &\leq \|\alpha(x, p^*) \nabla p^* + \alpha(x, p^*) \nabla(u - p^*) + (u - p^*) \alpha_s(x, p^*) \nabla p^* - \alpha(x, u) \nabla u\|_0 \\ &\leq \|\alpha(x, p^*) \nabla p^* + \mathcal{F}(p^*)(u - p^*) - \alpha(x, p^*) \nabla p^* - \mathcal{F}(p^*)(u - p^*) - \frac{(\alpha(x, q^*) \nabla q^*)_{uu}}{2} \\ &\quad \cdot (u - p^*)^2\|_0 \\ &\leq \|(\alpha(x, q^*) \nabla q^*)_{uu}\|_{\infty} \frac{\|u - p^*\|_0^2}{2}. \end{aligned}$$

Combining this estimate with the above-obtained error estimate finishes the proof.  $\square$

## 4 Numerical experiments

In this section, we test our multiscale method in two numerical experiments, illustrating the convergence with respect to the mesh size and the influence of the linearization strategy. The two experiments consider problem (2) with the same spatial multiscale coefficient, but different nonlinearities inspired by models for the stationary Richards equation, see [11]. We choose the computational domain  $\Omega = [0, 1]^2$  and the right-hand side  $f \in L^2(\Omega)$  as

$$f(x) = \begin{cases} 0.1 & \text{if } x_2 \leq 0.1, \\ 1 & \text{otherwise.} \end{cases}$$

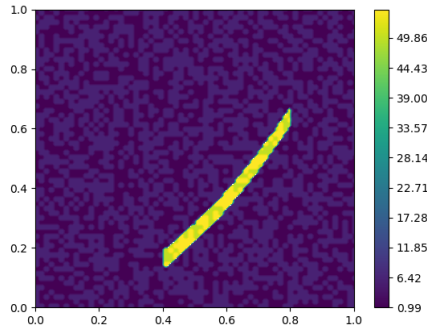


Figure 1: Spatial coefficient  $c(x)$

For the nonlinear diffusion coefficient, we choose  $\alpha(x, u) = c(x)k(u)$ , where the spatial part  $c$  is shown in Figure 1 and the model for  $k$  is given in each subsection. The spatial coefficient  $c$  is piecewise constant on a scale  $\varepsilon = 2^{-6}$  and exhibits a high-contrast channel. Our results are compared to a reference solution  $u_h \in V_h$  obtained using a standard FEM on a fine mesh of size  $h = 2^{-7}$ , which resolves all features of  $c$ . The local correction problems (12) are solved on the same fine mesh, cf. Remark 1. As an interpolation operator in the definition of  $W$ , we use the  $L^2$  projection. The coarse-scale mesh sizes are chosen as  $H = 2^{-1}, 2^{-2}, \dots, 2^{-6}$ . We emphasize that  $H$  generally does not resolve the fine-scale features of the solution  $u$ . For the implementation of the LOD method, we follow the algorithm in [15] with four different oversampling parameters  $k = 1, 2, 3, 4$ . The code is available at <https://github.com/Maherkh/LodNonmonotoneNonlinearPDE>. In particular, the linear space  $V_{H,k}$  is constructed only once, and then we solve the global nonlinear problem (13) iteratively. Precisely, we use the Kačanov iterative scheme with tolerance  $\text{tol} = 10^{-12}$  and starting value  $u_0 = p^*$ , where  $p^*$  is the linearization point used for the correction problems and is discussed below. In all experiments, this converged within the maximum of 10 iterations. In our experiments, we compare the performance of the two linearization methods introduced above and also study different linearization points  $p^*$  ranging from functions close to the analytical solution to functions further away from the analytical solution. Precisely, we consider the following options:

$$p^* = \begin{cases} 0, & \text{FEM coarse solution, } H = \frac{1}{32}, \\ u_H, & \text{FEM reference solution, } h = \frac{1}{128}, \\ u_h, & \text{LOD solution } H = \frac{1}{16} \text{ and } k = 4, \\ \text{ulod} \\ g(x) = 10xy(1-x)y(1-y), \\ g_1(x) = 0.5xy(1-x)y(1-y)e^{5(x+y)}. \end{cases}$$

We provide a brief explanation of the choices of  $p^*$  presented above. We use the coarse FEM solution  $u_H$  because we believe it holds some information about the analytical solution. However, the size of the mesh  $H$  does not recover the fine details of the analytical solution. Practically, the choice of the reference solution  $u_h$  should not be computed and used as a linearization point, but we use it here as a reference solution. However, it is used to investigate its impact on the linearization error. We tested the LOD solution  $p^* = \text{ulod}$  in order to check the effectiveness of an iterative LOD strategy on the improvement of the LOD discrete solution. Regarding  $g$  and  $g_1$ , we choose them arbitrarily such that  $g$  is of relatively small values and close to the solution. However,  $g_1$  is obtained by scaling  $g$  so that it deviates significantly away from the analytical solution. To study the convergence performance, we use the following relative errors

$$e_{\text{LOD}} := \frac{|u_h - u_{H,k}|_1}{|u_h|_1} \quad \text{and} \quad e_H := \frac{\|u_h - I_H u_{H,k}\|_0}{\|u_h\|_0},$$

called the relative upscaled error and the relative macroscopic error, respectively. According to Theorem 3 and Corollary 4, we expect  $e_{\text{LOD}}$  to converge linearly with respect to  $H$  and  $e_H$  to converge at the same rate as the  $L^2$ -best approximation error.

## 4.1 Exponential model

In our first experiment, we choose the so-called exponential model with  $k(u) = \exp(2u)$ . However, it is clear that  $\alpha(x, s)$  does not satisfy Assumption 1 for such model. Figure 2 shows the reference solution and an LOD approximation. Observe the influence of the high-contrast channel on the bottom right and the multiscale nature of both solutions arising from the rapid variations in  $c(x)$ . Both aspects are well captured by the LOD solution.

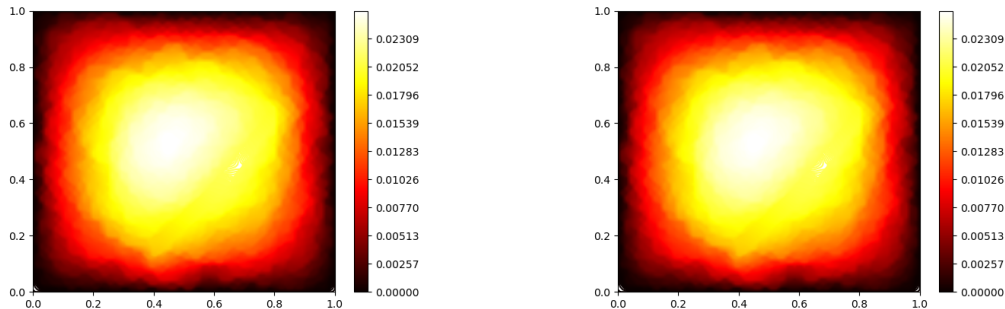


Figure 2: Reference solution (left) and LOD solution (right) obtained by Kačanov linearization method for  $H = 2^{-4}$  and  $k = 4$ .

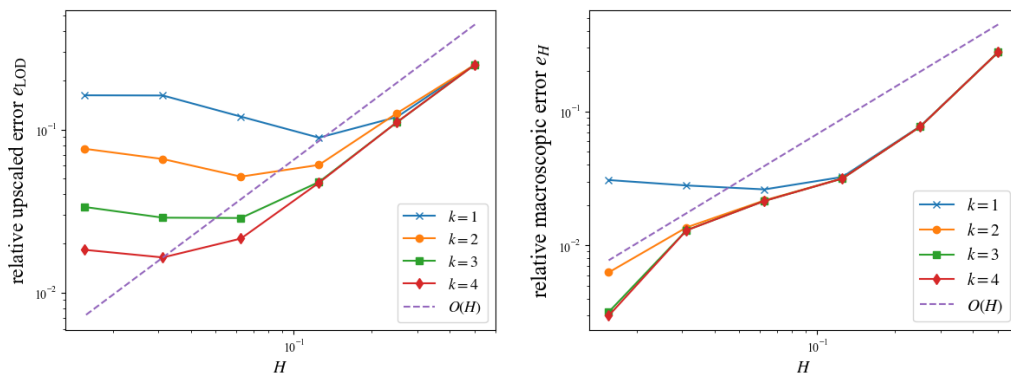


Figure 3: Convergence history of  $e_{\text{LOD}}$  (left) and  $e_H$  (right) for different oversampling parameters and fixed linearization point  $p^* = u_H$  using Fréchet linearization.

Figures 3 and 4 depict the convergence histories of our two error measures for the two linearization strategies and linearization point  $p^* = u_H$ . Regarding  $e_{\text{LOD}}$ , we observe the predicted convergence rate from Theorem 3. The saturation of the error curves corresponds to a domination of the localization error and sets in later for larger oversampling parameters, which perfectly agrees with Theorem 3 as well. Note that the overall convergence rate may even seem to be slightly better than linear convergence. We observe that the relative macroscopic errors  $e_H$  are very similar for all oversampling parameters  $k \geq 2$ . The convergence rate  $H$  corresponds to what we expect from Corollary 4 since we cannot hope for more than linear convergence of the  $L^2$ -best approximation due to the low regularity of the solution caused by the discontinuities in  $c$ . Comparing Figures 3 and 4, the two linearization strategies show almost the same performance. In particular, no impact of the linearization error is observed, probably because  $p^* = u_H$  is close enough to both solutions  $u$  and  $u_{H,k}$ . In Figure 5, we study the impact of different linearization points on the convergence history, for both linearization techniques. For the Kačanov technique, the choices  $p^* \in \{0, u_h, u_H, \text{ulod}\}$  all lead to very similar results, probably because all of them are close enough to the exact solution. Quantitatively, the choices  $p^* = \text{ulod}$  and  $p^* = u_h$  perform best by a slight margin. Surprisingly, when  $p^* = g$ , we obtain

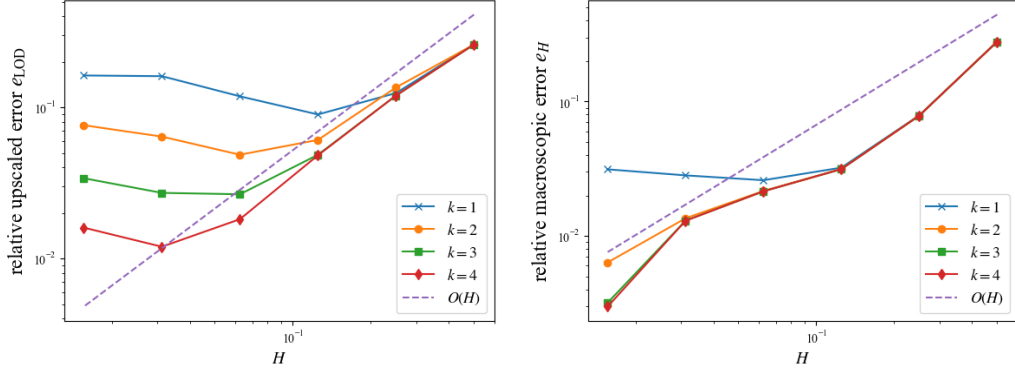


Figure 4: Convergence history of  $e_{\text{LOD}}$  (left) and  $e_H$  (right) for different oversampling parameters and fixed linearization point  $p^* = u_H$  using Kačanov method.

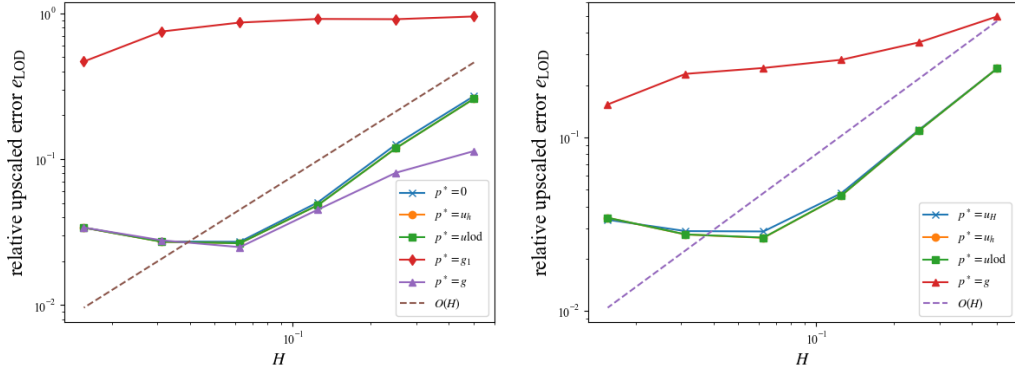


Figure 5: Convergence history of  $e_{\text{LOD}}$  for Kačanov method (left) and Fréchet method (right) with different linearization points and fixed oversampling parameter  $k = 3$ .

even slightly better results, in particular for large mesh sizes  $H$ . In contrast, using  $p^* = g_1$  leads to large error values, failing to reach the first order of convergence with respect to  $H$  due to the dominance of the linearization error. Finally, results for  $p^* = g_1$  are not depicted for the Fréchet technique, because the error values blows-up. This is in line with the theory as the condition  $C_I C_{p^*} H < 1$  is not satisfied where  $C_{p^*}$  is the constant imposed in the proof in Subsection 3.2. In this experiment, Fréchet linearization, hence, appears to be more sensitive with respect to the choice of the linearization point. It is important to emphasize that when using a linearization point that is close to the analytical solution, computing the correction only once seems to be sufficient, because no significant improvement is obtained when using  $p^* = ulod$ . For even better visibility of these observations, we compare Fréchet and Kačanov linearization for two different choices of  $p^*$  in one single Figure 6 (left). For  $p^* = u_h$ , we observe that both methods perform the same not only qualitatively but also quantitatively. The difference between Fréchet and Kačanov linearization goes to zero as the  $p^*$  gets closer to the exact solution, which explains this observation. In contrast, when  $p^* = g$ , as discussed above, we observe a significant impact of the linearization method on the convergence. The Fréchet technique is clearly performing worse, which is explained by the fact that  $\alpha_s(x, p^*) \nabla p^*$  becomes very large, so that the linearization error dominates the discretization error. In Figure 6 (right), we examine the Kačanov technique with  $p^* = g_1$  in more detail. We observed in Figure 5 that  $g_1$  is not a good choice and no convergence in the mesh size is obtained due to the large linearization error. However, taking the resulting bad LOD approximation as new linearization point  $p^*$ , the new LOD approximation recovers the expected convergence behavior. This shows the potential of iteratively computing

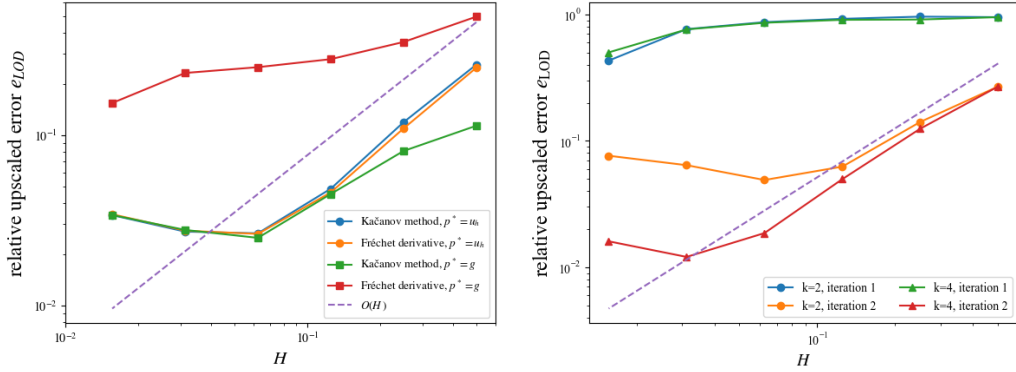


Figure 6: Convergence history of  $e_{LOD}$  using different linearization points,  $k = 3$ , with two different linearization methods (left), and for the iterative LOD (Right).

a whole cascade of LOD solutions.

## 4.2 Van Genuchten model

In our second experiment, we choose the nonlinearity according to the Van Genuchten model

$$k(u) = \frac{(1 + \alpha|u|(1 + (\alpha|u|)^2)^{-\frac{1}{2}})^2}{1 + (\alpha|u|)^2}, \quad \alpha = 0.005$$

and the spatial coefficient  $c(x)$  as above. This nonlinearity grows more slowly for  $|u| \rightarrow \infty$  than the exponential model and the values of  $k(u)$  even remain bounded. Consequently, we expect that, in particular, the condition  $C_I C_p^* H < 1$  for the Fréchet linearization is satisfied for more linearization points  $p^*$ . As for the exponential model, we observe the theoretically proved rates

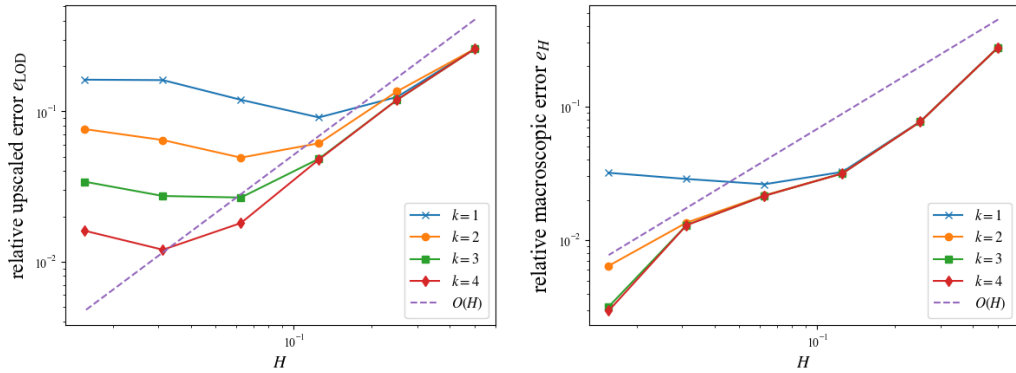


Figure 7: Convergence history of  $e_{LOD}$  (left) and  $e_H$  (right) for different oversampling parameters and fixed linearization point  $p^* = u_H$  using Fréchet linearization.

for  $e_H$  and  $e_{LOD}$  for both linearization strategies and  $p^* \in \{0, u_h, u_H, u_{lod}\}$ , cf. Figure 7, where the experiment is tested for  $p^* = u_H$ . As a main difference from the exponential model, we focus in the following on the influence of the linearization point, in particular when  $p^* = g$  or  $p^* = g_1$ . In Figure 8 (left), we observe that all linearization points perform qualitatively the same for the Kačanov technique. We especially emphasize that  $p^* = g_1$ , although having larger errors, now also shows the expected convergence rate in contrast to the exponential model. This different behavior is most probably due to the fact that  $k$  yields small values for various choices of  $p^*$  in the Van Genuchten model. In Figure 8 (right), we observe that all linearization points except for

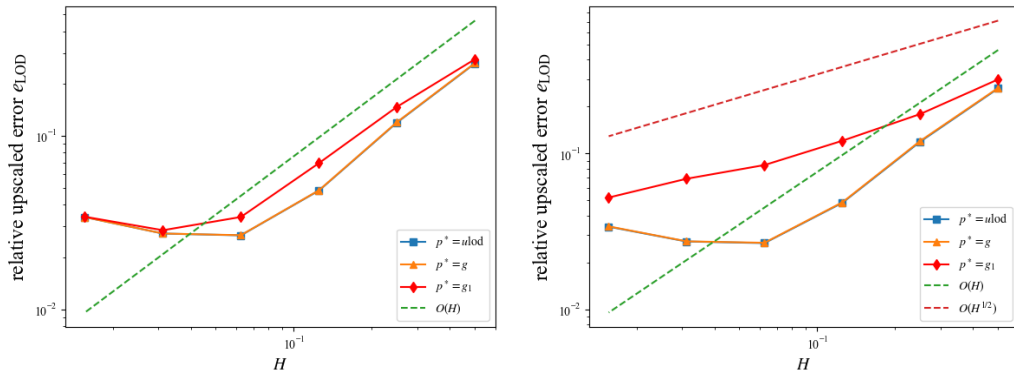


Figure 8: Convergence history of  $e_{\text{LOD}}$  for Kačanov method (left) and Fréchet method (right) with different linearization points and fixed oversampling parameter  $k = 3$ .

$g_1$  perform similar to the expected convergence rates also for the Fréchet linearization. Again, we emphasize the stark contrast to the exponential model, where now convergence in the mesh size occurs for  $p^* = g$ . The choice  $p^* = g_1$  still yields the largest errors for the Fréchet linearization, but we now observe a convergence with respect to  $H$ , which is approximately of order  $\frac{1}{2}$ . This is in great contrast to the exponential model, where the method does not even converge. Due to the smaller values of  $k$  in the Van Genuchten model, the condition  $C_I C_p^* H < 1$  appears to be satisfied here, but not for the exponential model as discussed above. To conclude, the Fréchet linearization still seems to be more sensitive with respect to the choice of  $p^*$ , but the smaller values of  $k(u)$  in the Van Genuchten model reduce this effect and, in general, make all results more robust with respect to the choice of  $p^*$ .

## Conclusion

We presented and analyzed a numerical homogenization method for a class of nonmonotone quasilinear problems with rapidly varying coefficient. Local correction problems are linearized by two linearization techniques in order to solve linear problems and construct a problem-adapted basis of low-dimension multiscale space. We proved the optimal error estimates for both linearization techniques. Numerical experiments illustrate the impact of the choice of the linearization points on the performance of the method. Some linearization points perform better than others, depending on how close they are to the analytical solution. The two linearization techniques especially differ when the linearization point is far from the solution. For the latter situation, an iteration of our multiscale method by updating the linearization point improves the performance considerably. This indicates that iterative multiscale methods in the spirit of [24, 21] may also be promising for nonmonotone quasilinear problems, which is left for future research.

## Acknowledgments

This work is funded by the Deutsche Forschungsgemeinschaft (DFG, German Research Foundation) under project number 496556642. BV also acknowledges support from the Deutsche Forschungsgemeinschaft (DFG, German Research Foundation) under Germany's Excellence Strategy – EXC-2047/1 – 390685813.

## References

- [1] Assyr Abdulle and Gilles Vilmart. A priori error estimates for finite element methods with numerical quadrature for nonmonotone nonlinear elliptic problems. *Numer. Math.*, 121(3):397–431, 2012.



- [2] Assyr Abdulle and Gilles Vilmart. Analysis of the finite element heterogeneous multiscale method for quasilinear elliptic homogenization problems. *Math. Comp.*, 83(286):513–536, 2014.
- [3] Robert Altmann, Patrick Henning, and Daniel Peterseim. Numerical homogenization beyond scale separation. *Acta Numer.*, 30:1–86, 2021.
- [4] N. André and M. Chipot. Uniqueness and nonuniqueness for the approximation of quasilinear elliptic equations. *SIAM Journal on Numerical Analysis*, 33(5):1981–1994, 1996.
- [5] J Bear and Y Bachmat. *Introduction to modeling of transport phenomena in porous media*. Boston, MA (US); Kluwer Academic Publishers, 1990.
- [6] Michel Chipot. *Elliptic equations: an introductory course*. Birkhäuser Advanced Texts: Basler Lehrbücher. [Birkhäuser Advanced Texts: Basel Textbooks]. Birkhäuser Verlag, Basel, 2009.
- [7] Jim Douglas and Todd Dupont. A galerkin method for a nonlinear dirichlet problem. *Mathematics of Computation*, 29(131):689–696, 1975.
- [8] Jim Douglas, Jr., Todd Dupont, and James Serrin. Uniqueness and comparison theorems for nonlinear elliptic equations in divergence form. *Arch. Rational Mech. Anal.*, 42:157–168, 1971.
- [9] Weinan E and Bjorn Engquist. The heterogeneous multi-scale method. In *Second International Congress of Chinese Mathematicians*, volume 4 of *New Stud. Adv. Math.*, pages 57–74. Int. Press, Somerville, MA, 2004.
- [10] Weinan E, Pingbing Ming, and Pingwen Zhang. Analysis of the heterogeneous multiscale method for elliptic homogenization problems. *J. Amer. Math. Soc.*, 18(1):121–156, 2005.
- [11] Y. Efendiev, J. Galvis, S. Ki Kang, and R. D. Lazarov. Robust multiscale iterative solvers for nonlinear flows in highly heterogeneous media. *Numer. Math. Theory Methods Appl.*, 5(3):359–383, 2012.
- [12] Y. Efendiev, T. Hou, and V. Ginting. Multiscale finite element methods for nonlinear problems and their applications. *Commun. Math. Sci.*, 2(4):553–589, 2004.
- [13] Yalchin Efendiev, Juan Galvis, and Thomas Y. Hou. Generalized multiscale finite element methods (GMsFEM). *J. Comput. Phys.*, 251:116–135, 2013.
- [14] Yalchin Efendiev, Juan Galvis, Guanglian Li, and Michael Presho. Generalized multiscale finite element methods. Nonlinear elliptic equations. *Commun. Comput. Phys.*, 15(3):733–755, 2014.
- [15] Christian Engwer, Patrick Henning, Axel Målqvist, and Daniel Peterseim. Efficient implementation of the localized orthogonal decomposition method. *Comput. Methods Appl. Mech. Engrg.*, 350:123–153, 2019.
- [16] N. Fusco and G. MoscarIELLO. On the homogenization of quasilinear divergence structure operators. *Ann. Mat. Pura Appl. (4)*, 146:1–13, 1987.
- [17] Patrick Henning, Axel Målqvist, and Daniel Peterseim. A localized orthogonal decomposition method for semi-linear elliptic problems. *ESAIM Math. Model. Numer. Anal.*, 48(5):1331–1349, 2014.
- [18] Ivan Hlaváček, Michal Krížek, and Jan Malý. On Galerkin approximations of a quasilinear nonpotential elliptic problem of a nonmonotone type. *J. Math. Anal. Appl.*, 184(1):168–189, 1994.
- [19] Thomas Y. Hou and Xiao-Hui Wu. A multiscale finite element method for elliptic problems in composite materials and porous media. *J. Comput. Phys.*, 134(1):169–189, 1997.
- [20] A. Karageorghis and D. Lesnic. Steady-state nonlinear heat conduction in composite materials using the method of fundamental solutions. *Comput. Methods Appl. Mech. Engrg.*, 197(33-40):3122–3137, 2008.
- [21] Xinliang Liu, Eric Chung, and Lei Zhang. Iterated numerical homogenization for multiscale elliptic equations with monotone nonlinearity. *Multiscale Model. Simul.*, 19(4):1601–1632, 2021.

- [22] Tina Mai, Siu Wun Cheung, and Jun Sur Richard Park. Constraint energy minimizing generalized multiscale finite element method for multi-continuum Richards equations. *J. Comput. Phys.*, 477:Paper No. 111915, 20, 2023.
- [23] Roland Maier. *Computational Multiscale Methods in Unstructured Heterogeneous Media*. doctoralthesis, Universität Augsburg, 2020.
- [24] Roland Maier and Barbara Verfürth. Multiscale scattering in nonlinear Kerr-type media. *Math. Comp.*, 91(336):1655–1685, 2022.
- [25] A. Målqvist and D. Peterseim. *Numerical homogenization by localized orthogonal decomposition*, volume 5 of *SIAM Spotlights*. Society for Industrial and Applied Mathematics (SIAM), Philadelphia, PA, 2021.
- [26] Kathrin Smetana and Tommaso Taddei. Localized model reduction for nonlinear elliptic partial differential equations: localized training, partition of unity, and adaptive enrichment. *SIAM J. Sci. Comput.*, 45(3):A1300–A1331, 2023.
- [27] Barbara Verfürth. Numerical homogenization for nonlinear strongly monotone problems. *IMA J. Numer. Anal.*, 42(2):1313–1338, 2022.